SPANDIDOS PUBLICATIONS

ONCOLOGY LETTERS 9: 2551-2559, 2015

^{1}H nuclear magnetic resonance-based extracellular metabolomic analysis of multidrug resistant Tca8113 oral squamous carcinoma cells

HUI WANG[1,2], JIAO CHEN[1], YUN FENG[1*], WENJIE ZHOU[1], JIHUA ZHANG[1], YU YU[1], XIAOQIAN WANG[1] and PING ZHANG[1*]

[1]State Key Laboratory of Oral Diseases, West China College of Stomatology, Sichuan University, Chengdu, Sichuan 610041; [2]Department of Stomatology, Tangshan Vocational and Technical College, Tangshan, Hebei 063004, P.R. China

Received June 26, 2014; Accepted March 19, 2015

DOI: 10.3892/ol.2015.3128

Abstract. A major obstacle of successful chemotherapy is the development of multidrug resistance (MDR) in the cancer cells, which is difficult to reverse. Metabolomic analysis, an emerging approach that has been increasingly applied in various fields, is able to reflect the unique chemical fingerprints of specific cellular processes in an organism. The assessment of such metabolite changes can be used to identify novel therapeutic biomarkers. In the present study, ^{1}H nuclear magnetic resonance (NMR) spectroscopy was used to analyze the extracellular metabolomic spectrum of the Tca8113 oral squamous carcinoma cell line, in which MDR was induced using the carboplatin (CBP) and pingyangmycin (PYM) chemotherapy drugs *in vitro*. The data were analyzed using the principal component analysis (PCA) and partial least squares discriminant analysis (PLS-DA) methods. The results demonstrated that the extracellular metabolomic spectrum of metabolites such as glutamate, glycerophosphoethanol amine, α-Glucose and β-Glucose for the drug-induced Tca8113 cells was significantly different from the parental Tca8113 cell line. A number of biochemicals were also significantly different between the groups based on their NMR spectra, with drug-resistant cells presenting relatively higher levels of acetate and lower levels of lactate. In addition, a significantly higher peak was observed at δ 3.35 ppm in the spectrum of the PYM-induced Tca8113 cells. Therefore, ^{1}H NMR-based metabolomic analysis has a high potential for monitoring the formation of MDR during clinical tumor chemotherapy in the future.

Correspondence to: Professor Ping Zhang or Professor Yun Feng, State Key Laboratory of Oral Diseases, West China College of Stomatology, Sichuan University, 14 (Section 3) South Renmin Road, Chengdu, Sichuan 610041, P.R. China
E-mail: pingzhang68@hotmail.com
E-mail: 953463551@qq.com

*Contributed equally

Key words: multidrug resistance, ^{1}H nuclear magnetic resonance, metabolomics, principal component analysis, partial least squares discriminant analysis

Introduction

Chemotherapy is important in the treatment of various human cancer types; however, numerous patients do not exhibit a satisfactory outcome following treatment (1,2). A major obstacle to successful chemotherapy is the development of multidrug resistance (MDR) in response to the treatment (1,2). An underlying mechanism of MDR is cellular overexpression of P-glycoprotein (P-gp), which is a 170-kDa transmembrane glycoprotein encoded by the *MDR1* gene, functioning as an efflux pump for numerous anticancer drugs (3). P-gp overexpresses on tumor cell surfaces, thus promoting the efflux of cytotoxic drugs out of these cells in an energy-dependent manner. Therefore, drug accumulation in the cells is reduced and MDR is increased. Upon the development of MDR, tumor cells are resistant to multiple chemotherapeutic drugs and reversing this process is difficult (4,5). A number of researchers have attempted to design novel approaches in order to monitor the development of MDR throughout the chemotherapeutic process (3,6,7).

Following the completion of the Human Genome Project, the biotechnology sector entered a novel, post-genomic era. Certain researchers emphasized on genomics, transcriptomics and proteomics, in succession; however, combining these methods did not provide answers to numerous important problems (8). A number of studies have attempted to develop novel approaches in order to explain these problems, giving rise to metabolomics, which may be a more comprehensive method for the interpretation of experimental data (9). Creating quantitative databases of metabolites may sufficiently reflect the metabolic systems in action and provide an understanding into how metabolism is functioning in each individual (10). Metabolomic analysis is applicable to various fields of biotechnology; although this method is novel, it has received increasing attention and its role in the post-genomic era is important. Metabolomics can provide a

chemical 'snapshot' of an organism's metabolic state through the measurement of small molecule metabolites (11,12).

Nuclear magnetic resonance (NMR) spectroscopy is a powerful tool in the rapidly growing field of metabolomics, since it does not damage the structure and nature of the samples and can be detected dynamically (13). Testing biological samples using NMR provides a large amount of information on various biomarkers. In order to fully extract the potential information in the data, chemometric and multivariate statistical analyses are required. Unsupervised principal component analysis (PCA) and supervised partial least squares discriminant analysis (PLS-DA) are the main methods used in this field (14). Previous studies have used PCA to investigate metabolic differentiation, as well as the description and recognition of the dynamic multivariate metabolism (14,15). Similarly, PLS-DA has been previously used for the analysis of metabolic changes (16). Currently, NMR-based metabolomics is applied in several fields, including the study of plants (17-19), blood plasma (20,21), urine (22) and cancer (23-26). In the present study, carboplatin (CBP) and pingyangmycin (PYM) were used to induce MDR of the oral squamous cell line, Tca8113, by applying an increasing concentration for a period of six months. The extracellular metabolic differences of drug resistant and parental cells were assessed by ^{1}H NMR-based metabolomic analysis to provide a novel approach for monitoring the development of MDR during chemotherapy.

Materials and methods

Drugs and chemicals. CBP was purchased from Qilu Pharmaceutical Co., Ltd. (Jinan, China), while PYM was obtained from Tianjin Taihe Pharmaceutical Co., Ltd. (Tianjin, China). In addition, paclitaxel (≥97%) was purchased from Sigma-Aldrich (St. Louis, MO, USA), doxorubicin was obtained from Shenzhen Main Luck Pharmaceuticals Inc. (Shenzhen, China), deuterium oxide (D_2O; ≥99.8%) was purchased from Norell®, Inc. (Landisville, NJ, USA), and fetal calf serum (FCS) was a product of Lanzhou National Hyclone Bio-Engineering Materials Co., Ltd. (Lanzhou, China). All the other chemicals were of the highest grade commercially available. Furthermore, drugs were adjusted to appropriate concentrations in the culture medium and stored at 0˚C until further use.

Cell culture. The human oral squamous carcinoma cell line, Tca8113, was obtained from the State Key Laboratory of Oral Diseases (Chengdu, China). Cells were cultured by seeding the culture flask (Corning® T-75; Corning Incorporated, Corning, NY, USA) at a density of 10^4 cells/ml in RPMI 1640 medium (Hyclone Laboratories, Logan, UT, USA), supplemented with 10% heat-inactivated FCS and penicillin/streptomycin (100 U/ml; GE Healthcare Life Sciences, Logan, UT, USA) in a humidified atmosphere of 5% CO_2 at 37˚C. The medium was refreshed every 2 or 3 days and the cells were trypsinized using 0.25% trypsin (GE Healthcare Life Sciences) and 0.02% EDTA when the cells reached 80-90% confluence. The FCS and other media used in this study were from the same batch.

In vitro selection of drug resistant Tca8113/CBP and Tca8113/PYM cells. The Tca8113 cell line was maintained in culture medium supplemented with 0.3 μg/ml CBP (Tca8113/CBP) or 0.3 μg/ml PYM (Tca8113/PYM) as the starting concentration. Upon reaching a density of $5x10^6$ cells/ml, the samples were resuspended in a 75 cm^2 culture flask and the drug dose was increased. After ~6 months and 40 passages, this intermittent means of increasing the drug concentration led to a final concentration of 10 μg/ml CBP and 5 μg/ml PYM.

Immunohistochemical analysis. Parental cells (Tca8113) and the chemotherapy resistant cell lines (Tca8113/CBP and Tca8113/PYM) were seeded at a density of $5x10^4$ cells/well in 6-well plates containing preplaced coverslips and grown for 72 h. The coverslips were fixed in 4% paraformaldehyde for 30 min, followed by 0.25% Triton X-100 (Amresco, LLC, Solon, OH, USA) for 15 min. Next, the samples were treated with 3% H_2O_2 for 30 min and rinsed three times in phosphate buffered saline (PBS; pH 7.4) for 5 min each time. The coverslips were then incubated with monoclonal mouse anti-human P-gp primary antibodies (1:100; cat. no. sc-13131; Santa Cruz Biotechnology, Inc., Dallas, TX, USA) in a humidified chamber at 37˚C for 2 h. Subsequent to washing with PBS, the coverslips were incubated with secondary polyclonal goat anti-mouse or anti-rabbit IgG (cat. no. SA1020; Wuhan Boster Biological Engineering Co., Ltd., Wuhan, China) antibodies for an additional 30 min at 37˚C. Finally, the cells were visualized using 3,3'-diaminobenzidine (Thermo Fisher Scientific Inc., Rockford, IL, USA) and lightly counterstained using Mayer's hematoxylin (Beijing Taize Technology Development Co., Ltd., Beijing, China). The coverslips were then mounted with Permount™ mounting medium (Thermo Fisher Scientific Inc., Fair Lawn, NJ, USA) and images were captured using a microscope (Eclipse 80i; Nikon Corporation, Tokyo, Japan) (3).

Drug sensitivity assay. Parental cells and the two chemotherapy resistant cell lines were seeded at a density of $2x10^4$ cells/well in 96-well plates. After culturing overnight, the medium was replaced with maintenance medium containing 10 μg/ml CBP, 5 μg/ml PYM, 2 nM paclitaxel and 4 μg/ml doxorubicin. Cell viability was assessed after 72 h using an MTT colorimetric assay. Briefly, the cells were washed with 300 μl PBS, followed by incubation with 20 μl MTT (5 mg/ml) in 200 μl RPMI 1640 medium at 37˚C for 3 h. The formazan product was dissolved in 200 μl dimethyl sulfoxide and quantified by measuring the optical absorbance (OA) at 570 nm using an ELISA plate reader (Thermo Electron Type 1500; Thermo Fisher Scientific Inc.). Cell viability was expressed as the percent ratio of $OA_{treated}$ vs. $OA_{untreared}$ control. Subsequently, the concentration curve was constructed by plotting the percentage of viable cells at each point against the drug concentration. The 50% inhibiting concentration (IC_{50}) values were calculated using linear regression analysis and IC_{50} values were considered to indicate the drug sensitivity, where low IC_{50} values indicate high drug sensitivity and high IC_{50} values indicate low drug sensitivity (3).

Extraction of extracellular metabolites. Parental cells and the two chemotherapy resistant cell lines were cultured at a density of $5x10^4$ cells/ml in a humidified atmosphere of 5% CO_2 at 37˚C. The medium was collected and centrifuged three times at 15,900 x g at 4˚C for 10 min after the cells reached 80-90% confluence. The supernatant (1 ml) and 0.5 ml 0.2 M sodium phosphate buffer were mixed and left to

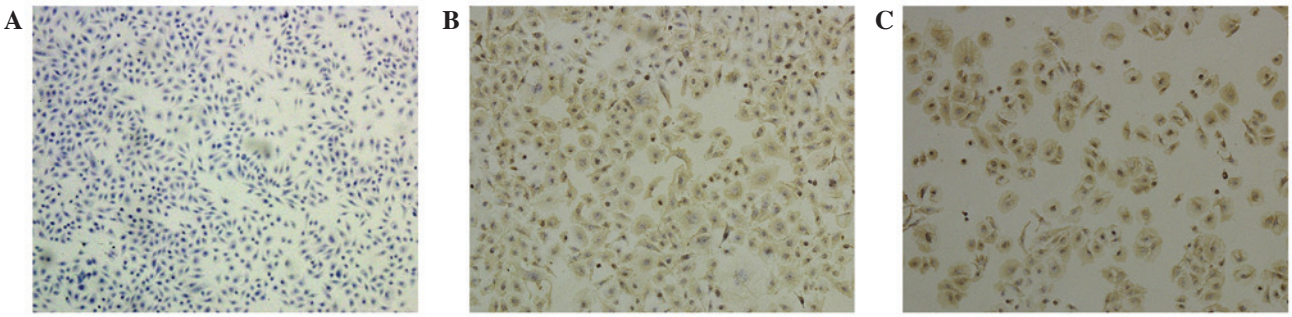

Figure 1. Immunostaining with P-gp. The parental Tca8113 cells were induced with increasing concentrations of CBP or PYM for six months. Cells were then stained by immunohistochemistry and visualized under magnification of x10 (stain, Mayer's hematoxylin). (A) Parental, (B) CBP-induced and (C) PYM-induced Tca8113 cells. The figures are representative of three independent experiments. P-gp, P-glycoprotein; CBP, carboplatin; PYM, pingyangmycin.

stand for 10 min at 4˚C. Next, a 500 μl mixture was reconstituted into 750 μl with D_2O (250 μl), following further centrifugation at 15,900 x g for 10 min at 4˚C. Subsequent to vortexing, each sample was imbibed for 500 μl and then pipetted into a 5 mm NMR tube. All the samples were stored at -80˚C prior to the ^{1}H NMR analysis.

^{1}H NMR spectroscopy. Data from the original free induction decay (FID) signal were acquired at 37˚C using a Bruker Avance II 600 spectrometer (Bruker Biospin GmbH, Rheinstetten, Germany), which was operated at 600.13 MHz with a 5-mm PATXI probe. The spectra were obtained using a pulse sequence (Bruker Biospin GmbH), which attenuated the broad protein signals in the samples, producing spectra with flat baselines. A Carr-Purcell-Meiboom-Gill (CPMG) pulse sequence modification was used in this study to suppress the residual water signal (27), and this sequence was CPMGPR1D.

Next, one-dimensional (1D) ^{1}H NMR spectra were collected for each sample, consisting of 64 K data points, 64 scans and 15-ppm spectral width. Further acquisition parameters included a 5-sec relaxation delay, 8 dummy scans, 400 μsec fixed echo time for elimination of J-mod and 400 CPMG loops for T2 filter (28). Subsequently, the NMR spectra acquired were manually corrected with lactate doublet as a reference at 1.33 ppm for the phase and baseline, using the TopSpin 1.3 software (Bruker Biospin GmbH).

These FID data were processed using MestReC software (version 4.8.1.1; Mestrelab Research, Santiago de Compostela, Spain) to obtain the original and satisfactory 1D NMR spectra by Fourier transformation, phase adjustment and baseline adjustment. Each ^{1}H NMR spectrum was automatically reduced to 242 integrated segments of equal width (0.04 ppm). Spectra with a range of 0.00-10.00 ppm, with the exception of residual water resonance (4.5-4.8 ppm), were segmented into 0.04 ppm wide bins, followed by importing the achieved integral values into Microsoft® Excel (Microsoft Corporation, Redmond, WA, USA).

PCA. PCA is an unsupervised analysis method that transforms multi-index into several irrelevant indicators by linear transformation using an idea of dimension reduction in order to reduce the complexity. The integral data were grouped and sorted, and then the spectral intensity was normalized to a unit area with the appropriate weighting coefficients in Microsoft® Excel spreadsheets prior to importing into the SIMCA-P v11.0 software package (Umetrics AB, Umeå, Sweden) for multivariate data analysis. PCA was conducted for the entire dataset using mean-centered data. The score plot revealed that the separation and clusters associated with the three groups: Tca8113 cells, Tca8113/CBP and Tca8113/PYM.

PLS-DA. PLS-DA, a variant of the partial least squares (PLS) regression, is a supervised chemometric method (29). PLS-DA indicated the presence of group separation, as well as helped establish whether the separation between the clusters was significant through the plots of PLS-DA coefficient and the variable influence on projection (VIP). This method is more advantageous compared with PCA, as it can reduce the noise of two blocks of variables, identify the missing data and handle the colinearity among the variables (30,31).

Statistical analysis. Data are expressed as the mean ± standard deviation. Statistical analysis of the results was performed using analysis of variance and post-hoc multiple comparison tests with the SPSS version 10.0 software (SPSS, Inc., Chicago, IL, USA). $P<0.05$ was considered to indicate a statistically significant difference.

Results

Immunohistochemical analysis. Compared with the parental cells (Fig. 1A), the drug-induced Tca8113/CBP and Tca8113/PYM cell lines expressed high levels of P-gp, which was loaded into the cytoplasm and membrane (Fig. 1B and C). In addition, the morphology of the drug-induced cells revealed an increased cytoplasmic area (Fig. 1)

Drug sensitivity of Tca8113 cells. Drug sensitivity was represented by the IC_{50} values. Drug-induced cells had a significantly higher IC_{50} value for the drugs compared with parental cells (Table I). Furthermore, these cells demonstrated primary-drug resistance, as well as cross-resistance. Therefore, considering the immunohistochemical results and IC_{50} values, these drug-induced cells appear to present MDR (Fig. 2; Table I).

Characteristics of the ^{1}H NMR spectra. The ^{1}H NMR spectra of the extracellular metabolites demonstrated abundant and significant information regarding the cell lines (Fig. 3). Regions of

Table I. Sensitivity of cell lines to anticancer drugs, observed by quantification of the drug IC_{50} values for the three cell lines.

	IC_{50} value		
Drug	Tca8113/ut	Tca8113/CBP	Tca8113/PYM
CBP (μg/ml)	6.99±0.34	22.63±0.15[a]	28.02±0.17[b,c]
PYM (μg/ml)	1.19±0.27	15.29±0.26[a]	14.16±0.08[b,c]
Paclitaxel (nM)	1.07±0.14	6.35±0.24[a]	4.69±0.11[b,c]
Doxorubicin (μg/ml)	3.54±0.13	4.48±0.19[a]	5.45±0.23[b,c]

[a]P<0.05 vs. Tca8113/ut; [b]P<0.05 vs. Tca8113/ut; [c]P<0.05 vs. Tca8113/CBP. Data are presented as the mean ± standard deviation of three independent experiments for each cell line. IC_{50}, 50% inhibiting concentration; ut, untreated; CBP, carboplatin; PYM, pingyangmycin.

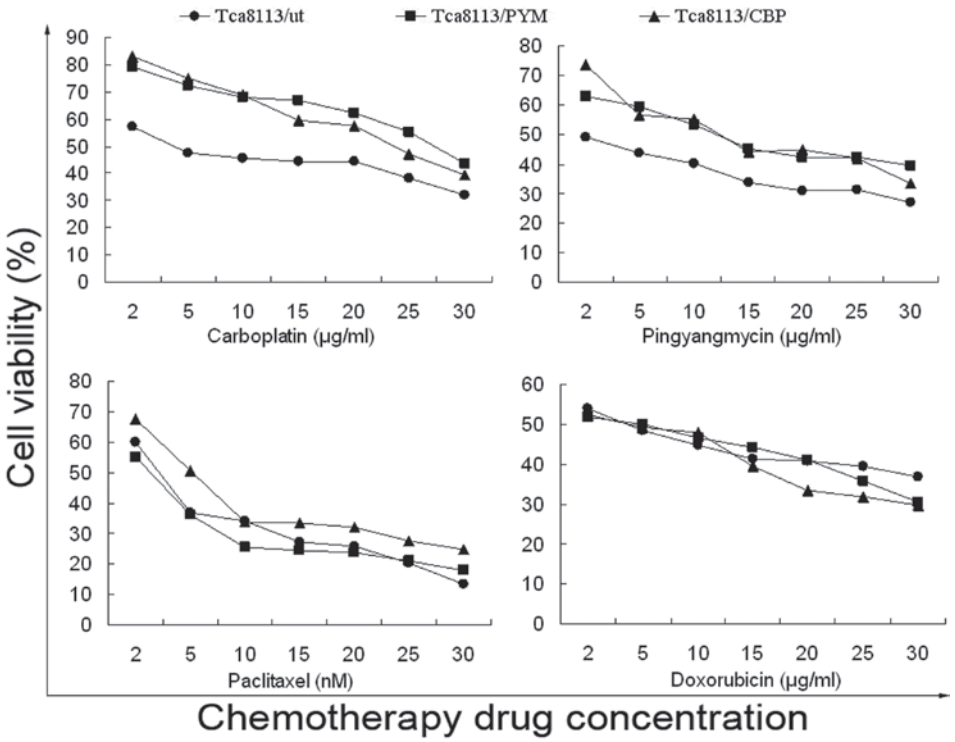

Figure 2. Drug sensitivity of Tca8113 cells against chemotherapeutic drugs. Dose-response curves for the three cell lines in the presence of chemotherapeutic drugs. Parental cells and chemotherapy-resistant Tca8113/CBP and Tca8113/PYM cell lines were treated with desired concentrations of chemotherapeutic drugs. Cell viability was assessed after 72 h using the MTT colorimetric assay. Data are presented as the mean ± standard deviation of three independent experiments. CBP, carboplatin; PYM, pingyangmycin.

most significant metabolite signals were typically in the range of δ 0-5.4 ppm, whereas the region of chemical shift δ 5.5-10.0 ppm revealed relatively weak signals. In addition, the acetate content was higher compared with the lactate levels in the drug-resistant cells (Fig. 3B and C); however, the opposite was true in the parental Tca8113 cells (Fig. 3A). The content of δ 3.35 ppm (arrow; Fig. 3C) was also relatively higher and this substance was tentatively identified as a type of myo-inositol (32). Studies regarding low-molecular weight metabolites have already been published (33,34). To further determine any differences between the drug-resistant and parental Tca8113 cells, specialized software was used for chemometric analysis.

PCA of extracellular metabolites. Subsequent to analyzing the data by PCA, new principal component (PC) variables were created, which explained >85% of the original data that were considered to be meaningful (Fig. 4A-C). The score plot obtained from the PCA displayed how the samples in the same group were situated with respect to each other. Adjacent observations were similar, while distant observations indicated their similarity was much worse. As shown in Fig. 4, the scores of PC1 and PC6, as well as of PC1 and PC4, were completely independent (Fig. 4A and B). However, the three cell lines were not completely separated using the PCA method (Fig. 4C). Thus, in order to obtain further information from the data, supervised PLS-DA was performed.

PLS-DA of extracellular metabolites. In total, six PLS components, which represented an R^2 value of 0.77 (original data) and a cross-validated R^2 value (Q^2) of 0.909, were obtained by

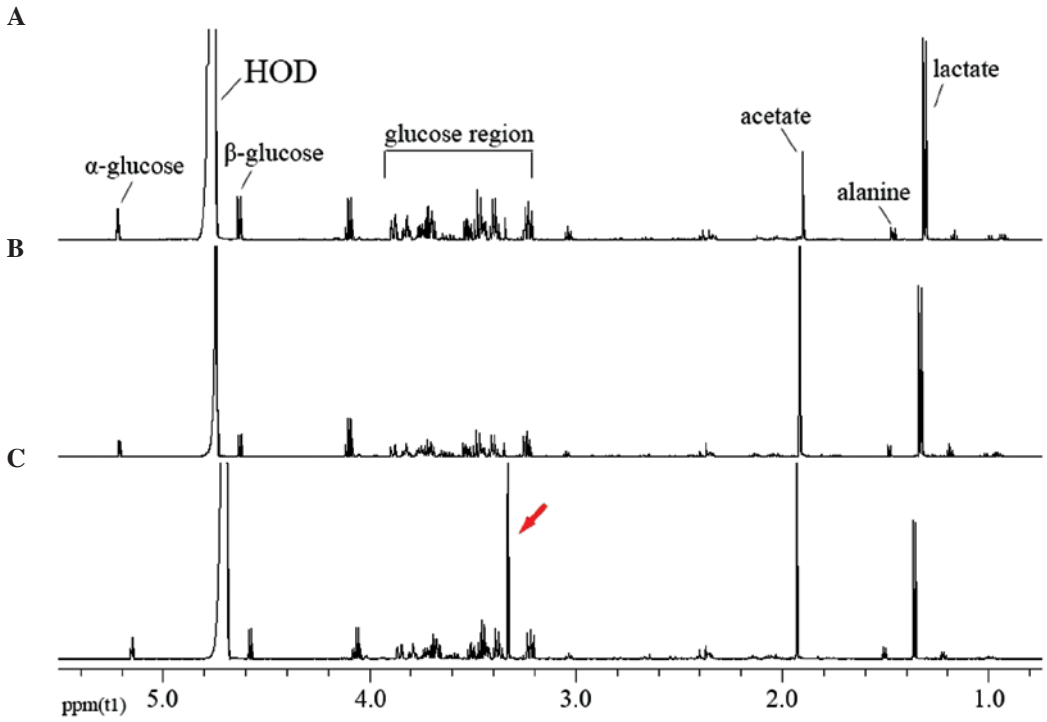

Figure 3. ^{1}H NMR spectra of extracellular metabolites of the three groups. (A) Parental, (B) CBP-induced and (C) PYM-induced Tca8113 cells. HOD, water/D_2O. NMR, nuclear magnetic resonance; CBP, carboplatin; PYM, pingyangmycin.

PLS-DA of the ^{1}H NMR spectra data for the three cell lines. An improved separation of the first two PLS components was observed (Fig. 5A) compared with the PCA (Fig. 4C) This result was also confirmed by the plot of the actual class value against the fitted class value (Fig. 5B), which demonstrated good separation between the different groups. The horizontal distance between the groups was an indicator of the group separation state (horizontal distance between the control and test groups, ~0.35; Fig. 5B). Considering the results of PCA (Fig. 4A and B), the drug-resistant cell lines and parental cells were found to be significantly separated. Notably, the two different drug-resistant cell lines were also found to be separated following PLS-DA (Fig. 6).

The VIP plot (Fig. 5C) depicts the most important regions of the ^{1}H NMR spectra. The VIP of each spectrum was normalized and the average squared VIP value was found to be 1; thus, a VIP value >1 in this model was considered sufficient for group discrimination. Fig. 5D shows the coefficient plot for the predictive component and indicates that variables are the key components that separate one cell line from the other. Along with the VIP plot, the variables play a key role in the separation of the three cell lines.

In addition, the validation plot (Fig. 5E) may be used to assess the risk of the PLS-DA model. The two regression lines display a correlation coefficient between the original Y and permuted Y vs. the cumulative R^2 and Q^2 values. R^2 describes how well the derived model fits the data, while Q^2, which is a proportion of R^2, describes the predictive ability of the derived model (35). A perfect model should have a high Q^2 value and an R^2 value that is lower compared with values at the original point on the upper right of the plot in Fig. 5E, indicating validation of the original model. The three dimensional score plot (Fig. 5F) dynamically reveals an enhanced cluster and separation of the three cell lines in the space.

A previous study (36) has demonstrated that the major regions of the NMR spectra for specific compounds were as follows: δ 0.598-1.022 ppm (methyl compounds), δ 1.056-1.286 ppm (methylene compounds), δ ~2.00 ppm (acetate), δ 3.200-3.90 ppm (glycosyl compounds), δ 3.21-3.23 ppm (choline compounds), δ 4.500-4.800 ppm (water peak) and δ 6.92-7.76 ppm (aromatic compounds). In the present study, the portion of extracellular metabolites (Table II) in PLS-DA was assigned by analyzing the VIP list obtained from the VIP plot and comparing the obtained chemical shifts with previously reported values (32,37-39). Table II depicts the corresponding chemical shifts of the identified metabolites, which presented VIP values of >1.

Discussion

MDR is a severe complication occurring during chemotherapeutic treatment of cancer and represents a major obstacle to successful therapy. Avoiding the development of MDR and reversing this effect once it is formed is difficult during the process of chemotherapy. A previously used strategy to counteract MDR was the increase of the drug or multi-drug combination doses; however, this results in a greater number of side-effects. Therefore, the implementation of novel approaches to monitor the development of MDR at the early stages of chemotherapy is crucial (4,5). During the dosing process in the present stduy, the passage number of drug-induced cells was ~40 times. Although the cell passage number has also been found to affect numerous of the cell line features, including growth in culture, viability and efflux protein expression (40), a certain passage range

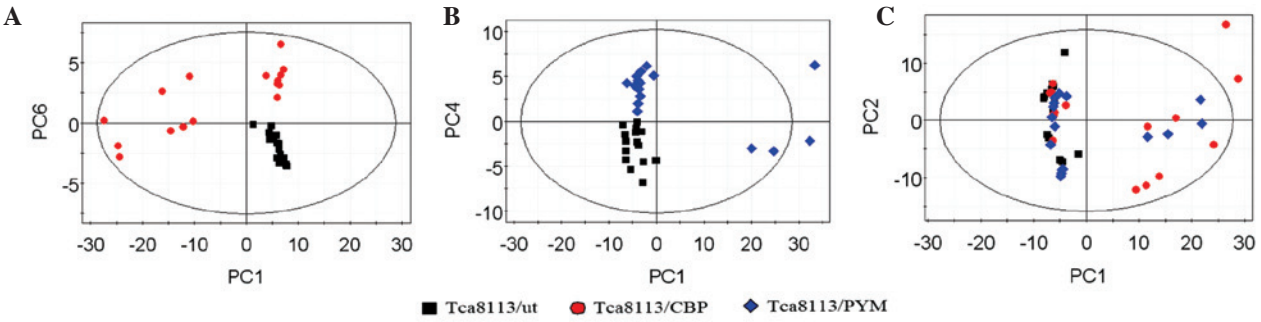

Figure 4. Score plots of PCA. (A) Plot of PC1 vs. PC6 from the parental cells and CBP-induced Tca8113 cells. (B) Plot of PC1 vs. PC4 from the parental cells and PYM-induced Tca8113 cells. (C) Plot of PC1 vs.PC2 from the parental cells, CBP-induced Tca8113 cells and PYM-induced Tca8113 cells. PCA, principal component analysis; PC, principal component; CBP, carboplatin; PYM, pingyangmycin.

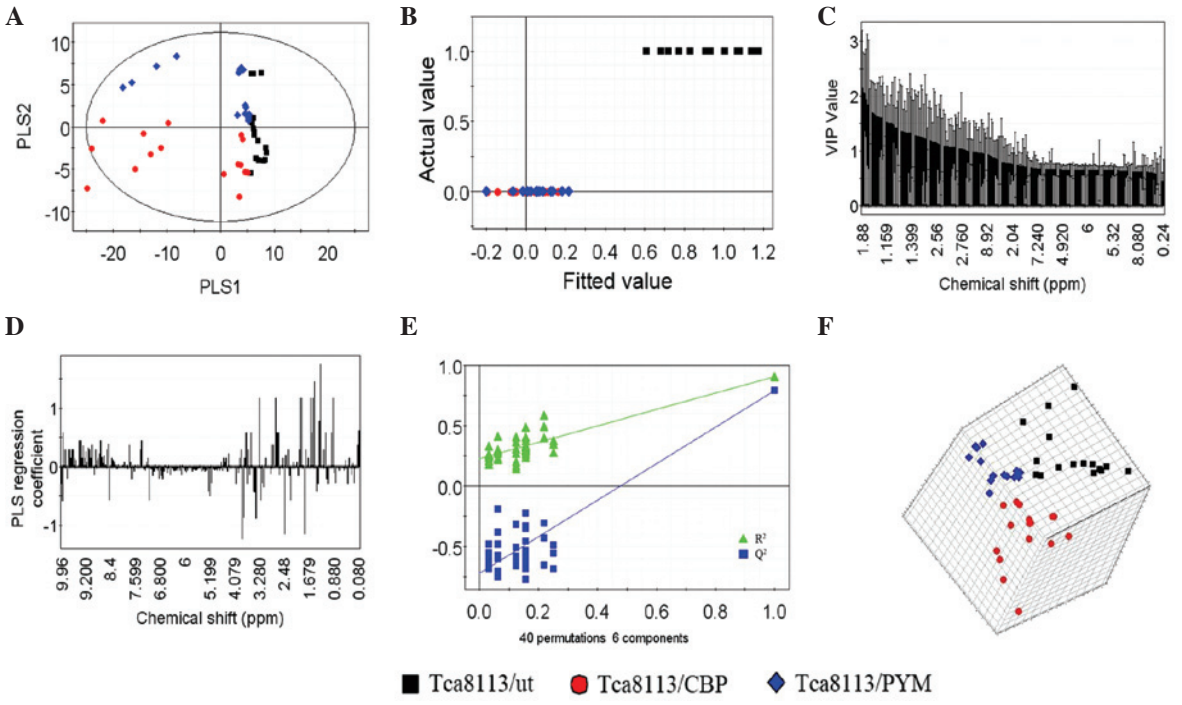

Figure 5. PLS-DA revealing the extracellular metabolomic differences of the three cell lines. (A) PLS1 vs. PLS2 plot of the three groups demonstrates strong separation. (B) Score plot of actual value against the fitted class value. (C) Plot of VIP. (D) Coefficient plot for the predictive component. (E) Internal validation of the aforementioned model. (F) Three dimensional score plot, demonstrating where the three groups were located in space. PLS-DA, partial least squares discriminant analysis; ut, untreated; CBP, carboplatin; PYM, pingyangmycin; VIP, variable influence on projection.

(such as passage 30-40) is normally used in laboratory experiments (41).

Metabolomics offers a platform for the development of scientific research (42). Pattern recognition and multivariate statistics are effective methods used to determine differences in cells, individuals and treatments (43,44). PCA and PLS-DA are two types of pattern recognition analyses. In the present study, these methods were used to analyze the extracellular metabolomic differences of parental Tca8113 cells and two chemotherapy resistant cell lines, Tca8113/CBP and Tca8113/PYM. The preliminary results revealed that the ^{1}H NMR-based metabolomic analysis was able to distinguish the drug-induced Tca8113 cell lines from the parental cells (Figs. 4 and 5). Furthermore, a strong separation was observed between the two drug-resistant cell lines (Fig. 6). During analysis, the CPMGPR1D pulse sequence was selected to filter the molecules with high metabolic concentration, since small molecule metabolites are likely to provide more pertinent information regarding an organism (45-47) and may potentially be novel biomarkers in cancer research.

The current study verified that the relatively high level of acetate and low level of lactate may play an important role in the drug resistance of cells (Fig. 3). Acetate is able to generate large numbers of HCO^{-}_{3}, which can counteract a portion of lactate, attenuating the toxicity caused by lactate (48). In addition, acetate may generate acetyl coenzyme A (CoA), which is involved in energy metabolism *in vivo* (49). Furthermore, the present study detected a significantly higher peak at δ 3.35 ppm in the spectrum of Tca8113/PYM (Fig. 3) and this metabolite was tentatively identified as a type of myo-inositol. Myo-inositol, which is synthesized from D-glucose (50), is the precursor of second messengers and the phospholipid synthesis (51,52). As previously reported, inositol derivatives are critical in membrane biogenesis, signal transduction and

Table II. Significant metabolites accountable for the discrimination of the three groups in the PLS-DA.

Metabolite	δ ^{1}H ppm (multiplicity[a])
Glutamate (bonded)	1.95, 3.78
Glutamate	2.15
Glycerophosphoethanol amine	4.11
Lactate	4.11, 1.33 (d)
α-Glucose	3.39, 3.71, 3.83 (ddd)
β-Glucose	3.47, 3.24 (d), 3.91 (dd)
Arginine	1.68, 3.24 (t), 3.79, 1.91
Acetate	1.91 (s)
Citrulline	1.87
Lysine	3.03 (t)
Lysine (bonded)	1.55
Methionine	3.87 (dd), 2.64 (t)
Phenylalanine	7.39 (m), 3.27 (dd), 7.42 (m)
Taurine	3.43 (t)
Proline	4.14
Proline (bonded)	3.83
Isoleucine	1.99, 1.27, 1.47 (s)
Threonine (bonded)	1.22 (d)
Threonine	3.59 (d)
Leucine	0.96 (d), 1.71 (m)
Creatine	3.03 (s)
Aspartate	2.81 (dd)
Formate	8.43 (s)
β-Hydroxybutyrate	1.20 (d)
Myo-inositol	3.62, 3.35, 3.56 (dd)
Serine	3.95 (dd)
Unsaturated Lipid	5.27
Alanine	1.46 (d), 3.78 (q)
Fatty acyl chain peak	1.59
Fucose	1.31 (d)
Lipid (mainly VLDL)	0.87 (t)
Polyamines	1.79
Isobutyrate	1.13 (d)
Albumin lysyl	2.99 (t)
2-Oxoglutarate	2.47 (t)
Trimethylamine	2.83 (s)
Glyceryl of lipids	5.20 (m)
Valine	0.99 (d), 1.04 (d)

[a]Chemical shifts were referenced against the ^{1}H shift of lactate (1.33 ppm). The listed metabolites had a VIP value >1. PLS-DA, partial least squares discriminant analysis; VIP, variable influence on projection; VLDL, very low-density lipoprotein; (s), singlet; (d), doublet; (dd), double doublet; (ddd), doublet of doublets of doublet; (t), triplet; (q), quartet; (m), complex multiplet.

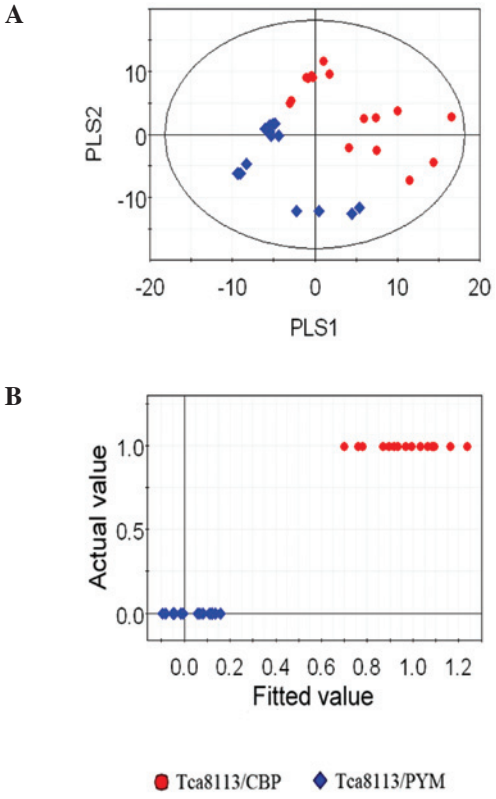

Figure 6. Score plots of the drug-resistant cells obtained following PLS-DA. (A) PLS1 vs. PLS2 plot of the drug-resistant cells. (B) Score plot of actual value against the fitted class value. PLS-DA, partial least squares discriminant analysis.

stress tolerance in plant cells (53). The increased content of inositol may also be an indicator sign of enhanced tolerance in drug-resistant tumor cells.

Furthermore, the present study demonstrated that metabolic differences not only exist between generate acetyl CoA, drug-resistant cells and parental cells, but also between the drug-resistant cells that are resistant to different types of drugs. This further illustrates why clinical chemotherapy often fails, since different drugs have different pharmacological and toxicological properties. In cells, these drugs may produce different metabolites and content changes of these metabolites may directly influence the physicochemical cellular properties. The three cell lines investigated in the current study exhibited certain significant metabolites accountable for discrimination, which had a VIP value >1. Thus, these findings support the hypothesis that these metabolites must be involved in the formation of MDR; however, the specific underlying mechanism requires further investigation.

In conclusion, the metabolic changes observed in the present study provide new clues for understanding the potential metabolic effects of chemotherapeutic drugs on disease. Future studies will investigate the metabolomic analysis of intracellular metabolites from these three groups. The ^{1}H NMR-based metabolomic technique is considered to have a significant value for the research of molecular disease properties. This novel technique has the potential of becoming a useful tool for early detection of tumor MDR in response to traditional chemotherapy.

Acknowledgements

This study was supported by a grant from the National Natural Science Foundation of China (no. 81372892).

References

1. Fardel O, Lecureur V and Guillouzo A: The P-glycoprotein multidrug transporter. Gen Pharmacol 27: 1283-1291, 1996.
2. Goldstein LJ: MDR1 gene expression in solid tumours. Eur J Cancer 32A: 1039-1050, 1996.
3. Chen J, Lu L, Feng Y, *et al*: PKD2 mediates multi-drug resistance in breast cancer cells through modulation of P-glycoprotein expression. Cancer Lett 300: 48-56, 2011.
4. Teodori E, Dei S, Scapecchi S and Gualtieri F: The medicinal chemistry of multidrug resistance (MDR) reversing drugs. Farmaco 57: 385-415, 2002.
5. Yan S, Ma D, Ji M, *et al*: Expression profile of Notch-related genes in multidrug resistant K562/A02 cells compared with parental K562 cells. Int J Lab Hematol 32: 150-158, 2010.
6. Varma MV, Ashokraj Y, Dey CS and Panchagnula R: P-glycoprotein inhibitors and their screening: a perspective from bioavailability enhancement. Pharmacol Res 48: 347-359, 2003.
7. Kars MD, Iseri OD, Gündüz U, Ural AU, Arpaci F and Molnár J: Development of rational in vitro models for drug resistance in breast cancer and modulation of MDR by selected compounds. Anticancer Res 26: 4559-4568, 2006.
8. Schmidt C: Metabolomics takes its place as latest up-and-coming''omic'' science. J Natl Cancer Inst 96: 732-734, 2004.
9. Ai JY, Smith B and Wong DT: Bioinformatics advances in saliva diagnostics. Int J Oral Sci 4: 85-87, 2012.
10. German JB, Bauman DE, Burrin DG, *et al*: Metabolomics in the opening decade of the 21st century building the roads to individualized health. J Nutr 134: 2729-2732, 2004.
11. Lindon JC, Holmes E and Nicholson JK: So what's the deal with metabonomics? Anal Chem 75: 384A-391A, 2003.
12. Ratajczak-Wrona W, Jablonska E, Antonowicz B, Dziemianczyk D and Grabowska SZ: Levels of biological markers of nitric oxide in serum of patients with squamous cell carcinoma of the oral cavity. Int J Oral Sci 5: 141-145, 2013.
13. Goodacre R, Vaidyanathan S, Dunn WB, Harrigan GG and Kell DB: Metabolomics by numbers: acquiring and understanding global metabolite data. Trends Biotechnol 22: 245-252, 2004.
14. Nicholson JK, Lindon JC and Holmes E: 'Metabonomics': understanding the metabolic responses of living systems to pathophysiological stimuli via multivariate statistical analysis of biological NMR spectroscopic data. Xenobiotica 29: 1181-1189, 1999.
15. Bathen TF, Jensen LR, Sitter B, *et al*: MR-determined metabolic phenotype of breast cancer in prediction of lymphatic spread, grade and hormone status. Breast Cancer Res Treat 104: 181-189, 2007.
16. Pec J, Flores-Sanchez IJ, Choi YH and Verpoorte R: Metabolic analysis of elicited cell suspension cultures of *Cannabis sativa* L. by ^{1}H-NMR spectroscopy. Biotechnol Lett 32: 935-941, 2010.
17. Seger C and Sturm S: Analytical aspects of plant metabolite profiling platforms: current standings and future aims. J Proteome Res 6: 480-497, 2007.
18. Kim HK, Choi YH and Verpoorte R: NMR-based metabolomic analysis of plants. Nat Protoc 5: 536-549, 2010.
19. Allwood JW, Clarke A, Goodacre R and Mur LA: Dual metabolomics: a novel approach to understanding plant-pathogen interactions. Phytochemistry 71: 590-597, 2010.
20. Sheedy JR, Ebeling PR, Gooley PR and McConville MJ: A sample preparation protocol for ^{1}H nuclear magnetic resonance studies of water-soluble metabolites in blood and urine. Anal Biochem 398: 263-265, 2010.
21. Barton RH, Waterman D, Bonner FW, *et al*: The influence of EDTA and citrate anticoagulant addition to human plasma on information recovery from NMR-based metabolic profiling studies. Mol Biosyst 6: 215-224, 2010.
22. Holmes E, Nicholls AW, Lindon JC, *et al*: Development of a model for classification of toxin-induced lesions using ^{1}H NMR spectroscopy of urine combined with pattern recognition. NMR Biomed 11: 235-244, 1998.
23. Beckonert O, Monnerjahn J, Bonk U and Leibfritz D: Visualizing metabolic changes in breast-cancer tissue using ^{1}H-NMR spectroscopy and self-organizing maps. NMR Biomed 16: 1-11, 2003.
24. Yokota H, Guo J, Matoba M, Higashi K, Tonami H and Nagao Y: Lactate, choline and creatine levels measured by vitro ^{1}H-MRS as prognostic parameters in patients with non-small-cell lung cancer. J Magn Reson Imaging 25: 992-999, 2007.
25. Griffin JL and Kauppinen RA: Tumour metabolomics in animal models of human cancer. J Proteome Res 6: 498-505, 2007.
26. Tiziani S, Lopes V and Günther UL: Early stage diagnosis of oral cancer using ^{1}H NMR-based metabolomics. Neoplasia 11: 269-276, 2009.
27. Lucas LH, Larive CK, Wilkinson PS and Huhn S: Progress toward automated metabolic profiling of human serum: comparison of CPMG and gradient-filtered NMR analytical methods. J Pharm Biomed Anal 39: 156-163, 2005.
28. Levitt MH: Spin Dynamics. Basics of Nuclear Magnetic Resonance. 2nd edition. John Wiley & Sons, New York, NY, 2008.
29. Jackson JE: A User's Guide to Principal Components. John Wiley & Sons, Inc., New York, NY, pp20-150, 1991.
30. Zhou J, Xu B, Huang J, *et al*: ^{1}H NMR-based metabonomic and pattern recognition analysis for detection of oral squamous cell carcinoma. Clin Chim Acta 401: 8-13, 2009.
31. Gavaghan CL, Wilson ID and Nicholson JK: Physiological variation in metabolic phenotyping and functional genomic studies: use of orthogonal signal correction and PLS-DA. FEBS Lett 530: 191-196, 2002.
32. Rocha CM, Barros AS, Gil AM, *et al*: Metabolic profiling of human lung cancer tissue by ^{1}H high resolution magic angle spinning (HRMAS) NMR spectroscopy. J Proteome Res 9: 319-332, 2010.
33. Tang H, Wang Y, Nicholson JK and Lindon JC: Use of relaxation-edited one-dimensional and two-dimensional nuclear magnetic resonance spectroscopy to improve detection of small metabolites in blood plasma. Anal Biochem 325: 260-272, 2004.
34. Ala-Korpela M: ^{1}H NMR spectroscopy of human blood plasma. Prog Nucl Magn Reson Spectrosc 27: 475-554, 1995.
35. Wang L, Chen J, Chen L, *et al*: 1H-NMR based metabonomic profiling of human esophageal cancer tissue. Mol Cancer 12: 25, 2013.
36. Lenz EM, Bright J, Wilson ID, Morgan SR and Nash AF: A ^{1}H NMR-based metabonomic study of urine and plasma samples obtained from healthy human subjects. J Pharm Biomed Anal 33: 1103-1115, 2003.
37. Nicholson JK, Foxall PJ, Spraul M, Farrant RD and Lindon JC: 750 MHz ^{1}H and ^{1}H-13C NMR spectroscopy of human blood plasma. Anal Chem 67: 793-811, 1995.
38. Ulrich EL, Akutsu H, Doreleijers JF, *et al*: BioMagResBank. Nucleic Acids Res 36 (Database): D402-D408, 2008.
39. Wishart DS, Tzur D, Knox C, *et al*: HMDB: The human metabolome database. Nucleic Acids Res 35 (Database): D521-D526, 2007.
40. Briske-Anderson MJ, Finley JW and Newman SM: The influence of culture time and passage number on the morphological and physiological development of Caco-2 cells. Proc Soc Exp Biol Med 214: 248-257, 1997.
41. Siissalo S, Laitinen L, Koljonen M, *et al*: Effect of cell differentiation and passage number on the expression of efflux proteins in wild type and vinblastine-induced Caco-2 cell lines. Eur J Pharm Biopharm 67: 548-554, 2007.
42. Goldsmith P, Fenton H, Morris-Stiff G, Ahmad N, Fisher J and Prasad KR: Metabonomics: A useful tool for the future surgeon. J Surg Res 160: 122-132, 2010.
43. Holmes E, Foxall PJ, Nicholson JK, *et al*: Automatic data reduction and pattern recognition methods for analysis of ^{1}H nuclear magnetic resonance spectra of human urine from normal and pathological states. Anal Biochem 220: 284-296, 1994.
44. Fauvelle F, Dorandeu F, Carpentier P, *et al*: Changes in mouse brain metabolism following a convulsive dose of soman: a proton HRMAS NMR study. Toxicology 267: 99-111, 2010.
45. Schroeder FC: Small molecule signaling in Caenorhabditis elegans. ACS Chem Biol 1: 198-200, 2006.
46. Schroeder FC, Gibson DM, Churchill AC, *et al*: Differential analysis of 2D NMR spectra: New natural products from a pilot-scale fungal extract library. Angew Chem Int Ed Engl 46: 901-904, 2007.
47. Bédouet L, Rusconi F, Rousseau M, *et al*: Identification of low molecular weight molecules as new components of the nacre organic matrix. Comp Biochem Physiol B Biochem Mol Biol 144: 532-543, 2006.
48. Vinay P, Prud'Homme M, Vinet B, *et al*: Acetate metabolism and bicarbonate generation during hemodialysis: 10 years of observation. Kidney Int 31: 1194-1204, 1987.
49. Zhu Y, Eiteman MA, Lee SA and Altman E: Conversion of glycerol to pyruvate by Escherichia coli using acetate- and acetate/glucose-limited fed-batch processes. J Ind Microbiol Biotechnol 37: 307-312, 2010.
50. Meng PH, Raynaud C, Tcherkez G, *et al*: Crosstalks between myo-inositol metabolism, programmed cell death and basal immunity in Arabidopsis. PLoS One 4: e7364, 2009.

51. Downes CP, Gray A and Lucocq JM: Probing phosphoinositide functions in signaling and membrane trafficking. Trends Cell Biol 15: 259-268, 2005.
52. Malan TP Jr and Porreca F: Lipid mediators regulating pain sensitivity. Prostaglandins Other Lipid Mediat 77: 123-130, 2005.
53. Loewus FA and Murthy PP: Myo-Inositol metabolism in plants. Plant Sci 150: 1-19, 2000.